



Short communication

Electrochemical behaviors of Si/C composite synthesized from F-containing precursors

Y. Liu^{a,*}, Z.Y. Wen^a, X.Y. Wang^a, A. Hirano^b, N. Imanishi^b, Y. Takeda^b^a Shanghai Institute of Ceramics, Chinese Academy of Sciences, 1295 Ding Xi Road, Shanghai 200050, China^b Department of Chemistry, Faculty of Engineering, Mie University, Kamihama-cho, Tsu, Mie 514-8507, Japan

ARTICLE INFO

Article history:

Received 2 July 2008

Received in revised form 11 August 2008

Accepted 11 August 2008

Available online 19 August 2008

Keywords:

Si/C composite

Negative electrode materials

Lithium-ion batteries

Morphological stability

Pyrolysis

ABSTRACT

Blends of silicon with various organic precursors were pyrolyzed for constructing the Si-containing disordered carbon and the effects of the amorphous carbon on the electrochemical performances of the resulting Si/C composites were investigated. It was found that the pyrolysis of poly(vinylidene fluoride) provided an appropriate carbon matrix to suppress the pulverizing of Si by the volume changes during lithium intercalation and extraction. Accordingly, nanosized Si was dispersed within the pyrolyzed poly(vinylidene fluoride). The porous composite exhibited a specific capacity of approximately 660 mAh g⁻¹ with a 75% capacity retention after 50 cycles. The cycling stability is a substantial improvement over nanosized silicon where a rapid drop in capacity occurred within a few cycles.

© 2008 Elsevier B.V. All rights reserved.

1. Introduction

Alloys that can electrochemically absorb lithium are promising anode candidates for Li-ion batteries. In particular silicon is of special interest due to a very high theoretical capacity of ca. 4008 mAh g⁻¹ for the formation of the Li₂₂Si₄ alloy. However, the volume changes accompanying lithium alloying generally generate a strongly mechanical stress in the host, which leads to a rapid capacity fade. To conquer these problems current researches are focusing on the elaboration of composite materials associating metallic nanoparticles dispersed in various conductive matrixes. Disordered carbon prepared by the pyrolysis of various organic precursors provides an effective matrix for silicon due to the small volume expansion of carbon on lithium intercalation (ca. 9% for graphite) and the ability of the ductile carbon to accommodate the volume change of silicon, reducing mechanical strain within the electrode and consequent electrode disintegration. The first report by Dahn's group showed that by pyrolyzing siloxane polymer or blends of pitch and polysiloxane, silicon could be incorporated into carbon at atomic scale. The composites had a stable capacity of ca. 500 mAh g⁻¹ [1,2]. So far, various organic precursors, such as polystyrene resin, carbon aerogel, pitch, polyparaphenylene, polyvinyl chloride (PVC) and so on, have been investigated

for the pyrolyzed carbon [3–8]. Compared to the thermal vapor deposition [9–11], the pyrolysis is a cost-effective method for the production of the Si/C composites in large quantities. The most adoptive structure of the Si/C composites seems to be high dispersion of nanosized silicon in the carbon matrix. Additionally, to a great extent the organic precursors for pyrolysis present a key [12–14].

Aim of this work was thus to find a suitable precursor for the pyrolyzed Si/C composite. Pyrolysis of poly(vinylidene fluoride) (PVDF) was found to have a strongly constructive influence to the active Si, leading to an obvious improvement of the cycling stability of Si.

2. Experimental

2.1. Preparations of the Si/C composites

The organic precursors for pyrolysis were selected on the basis of poly(vinylidene fluoride), sucrose, chlorinated polyethylene (CPE), polyvinyl chloride, polyethylene (PE), resin, polyethylene oxide (PEO) and pitch (mesophase). The Si particles with average size of approximately 1 μm (>99.8%) and 60 nm were commercially available. A given amount of the precursors and the silicon (1 μm) was homogeneously mixed by ball-milling for 30 min. The mixtures were pyrolyzed at 900 °C in an Ar/H₂ (4% H₂) atmosphere for 1 h. The heating rate was 10 °C h⁻¹. The pyrolysis was allowed to be cooled naturally. The resulting samples were ground. Thermal

* Corresponding author. Tel.: +86 21 5241 2272; fax: +86 21 5241 3903.

E-mail addresses: yuliu@mail.sic.ac.cn, yuliu518@hotmail.com (Y. Liu).

behaviors of the precursors were measured by thermogravimetric (TG) analysis using Mac Science 5000S system in the temperature range of 30–900 °C with a heating rate of 2 °C min⁻¹ in Ar/H₂ (4% H₂) atmosphere. The nanostructured Si/C composites were obtained by adding nanosized Si (60 nm) into the PVDF (dissolved in tetrahydrofuran solution) and homogeneously mixed under ultrasonic action. The solvent was evaporated under stirring to get a solid blend. The blend was then gradually heated to 900 °C under Ar/H₂ (4% H₂) atmosphere. After pyrolysis at 900 °C for 1 h, the furnace was cooled automatically. The products were further ground. Powder X-ray diffraction (XRD) patterns were obtained using automated powder diffractometer with Cu K α radiation (Rotaflex RU-200B, Rigaku-denki Corporation). The morphological characterization of the materials was characterized with scanning electron microscopy (SEM) and transmission electron microscopy (TEM).

2.2. Electrochemical measurements

A normal casting was used for preparing the Si and Si/C composites based electrodes. The electrodes contain 8 wt.% acetylene black (AB), 80 wt.% active materials and 12 wt.% poly(vinylidene fluoride). The active powders and AB were homogeneously mixed in a 0.02 g mL⁻¹ PVDF/1-methyl-2-pyrrolidone (NMP) solution, and the viscous mixture was cast onto a 300- μ m thick Ni foam, which served as a current collector. The electrode was further dried at 120 °C under vacuum for 2 h until NMP solvent was entirely removed. After being pressed at 300 kgf cm⁻², the geometric area of the electrodes was 1.0 cm², and the typical thickness was 190–200 μ m.

To evaluate the electrochemical properties of the electrodes, a half-cell containing LiClO₄/EC+DMC (ethylene carbonate plus diethyl carbonate as 1:1 in volume) electrolyte was used, and lithium metal was utilized as the counter electrode. All the three layers, including test electrode, separator and lithium metal, were stacked in a 2025 coin type cell in a glove box. Unless stated elsewhere, cycling was carried out at a constant current density of 0.18 mA mg⁻¹ and a voltage cutoff at 1.5/0.02 V vs. Li/Li⁺. Charge and discharge of the cell refer, respectively, to lithium extraction from, and insertion into, the active hosts. Electrode capacity was calculated according to the weight of active materials.

3. Results and discussion

Fig. 1 shows XRD patterns of the Si/C composites prepared by the pyrolysis of the blends of Si with various precursors at 900 °C in Ar/H₂ (4% H₂) for 1 h. As can be seen, pyrolysis of the organic precursors included in this study mainly obtained the disordered

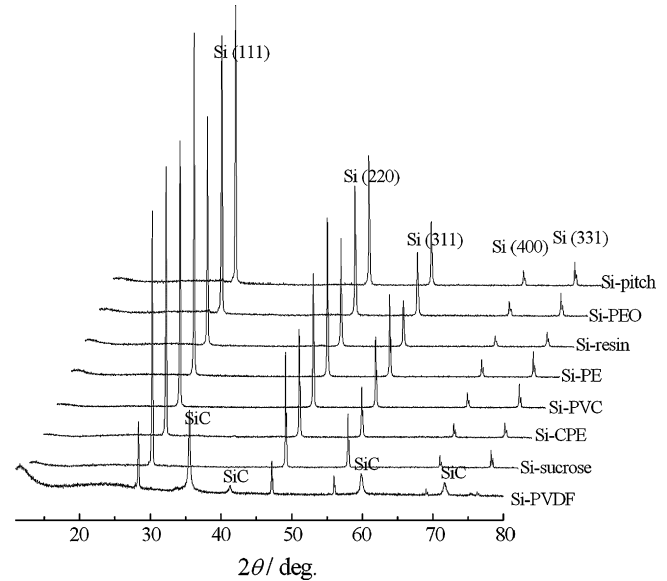


Fig. 1. XRD patterns of the products by pyrolysis of blends of silicon with various organic precursors at 900 °C in Ar/H₂ (4% H₂).

carbon, which presented the amorphous structures. The typically crystalline reflections corresponding to the active Si were obvious for most of the products, whereas some new phases relating to the inert silicon carbide (SiC) were observed for the pyrolyzed Si–PVDF composite. In general, the formation of the inert SiC phase occurs at 1300 °C and above, partially because of the complete removal of oxygen in the pyrolyzed carbon [1,2]. The complete formation of the inert silicon carbide may finally lose the electrochemical activity of Si. A good review respecting to the influence of the SiC reaction on the electrochemical behavior of the Si/C composites has been recently given by Dahn and coworkers [15].

To further analyze the Si/C reaction, the XRD patterns of the pyrolyzed products of the Si/sucrose and Si/PVDF mixtures were compared as a function of the temperatures. Reflection peaks and positions of the Si, SiC and amorphous carbon phases were highlighted. As shown in Fig. 2a, no silicon carbide phase was observed for the pyrolyzed Si/sucrose composite until 1300 °C. The results are highly consistent with most reports of the pyrolyzed Si/C systems [3–8], in which the temperatures of pyrolysis could be generally set in the ranges of 700–1200 °C without the formation of the inert SiC phase. In contrast, the silicon carbide reaction started at a relatively low temperature of 700 °C for the Si/PVDF composite and

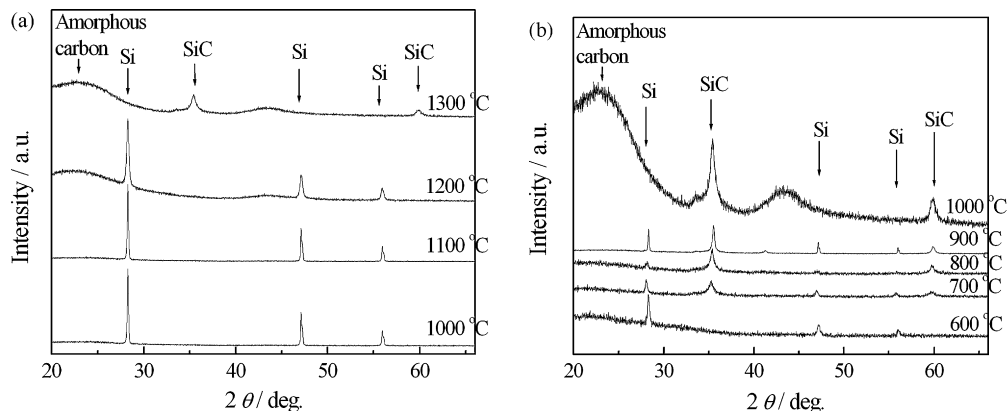


Fig. 2. XRD patterns of the products by pyrolysis of the (a) Si/sucrose and (b) Si/PVDF mixtures as a function of temperature in Ar/H₂ (4% H₂).

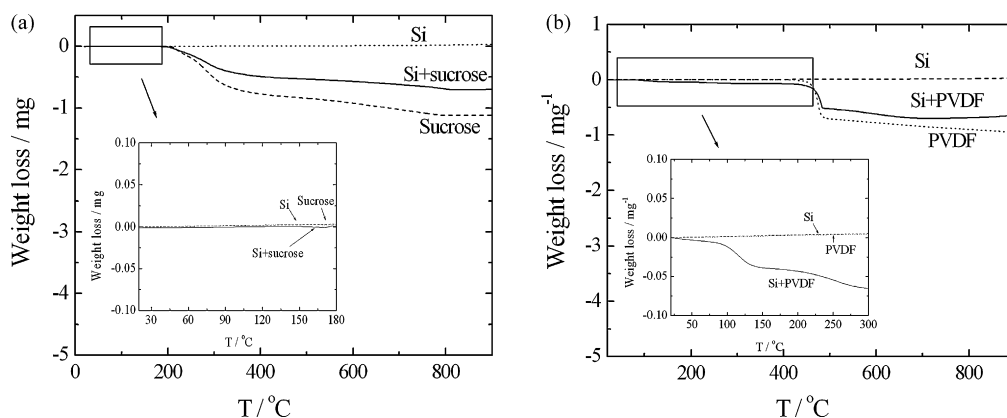


Fig. 3. Thermogravimetric (TG) curves of (a) the Si/sucrose and (b) Si/PVDF mixtures from 30 to 900 °C at heat rate of 2 °C min⁻¹ in Ar/H₂ (4% H₂).

the SiC phases coexisted with Si until 900 °C, as shown in Fig. 2b. At 1000 °C, no peaks corresponding to the crystalline Si were further observed. The phenomenon was considered to be mainly the influence of the chemical compositions like C, H, O or F included in the pyrolyzed carbon [1,2,16].

The thermal behaviors of the Si/sucrose and the Si/PVDF mixtures measured by the thermogravimetric analysis at 30–900 °C in Ar/H₂ were shown in Fig. 3. The decomposition started at approximately 160 °C for sucrose (Fig. 3a) and 360 °C for PVDF (Fig. 3b), respectively. This contributed to the main weight loss of the mixtures during the pyrolysis. As can be seen, the weight changes of pure Si did not follow the increase of temperature and those of PVDF and sucrose remained almost unchangeable before their decompositions. Inset of the figures further showed the thermal behaviors of the mixtures before the decompositions of the organic precursors. No weight change was observed for the Si/sucrose mixture prior to the decomposition of sucrose, as shown in Fig. 3a. In contrast, the weight of the Si/PVDF mixture suffered from an obvious loss before the decomposition of PVDF, as shown in Fig. 3b. Fluorine (F) is well known to have a strong etching effect on silicon. Insertion of F into Si–Si bonds becomes possible because of relaxed steric constraints in the near-surface region [17]. The weight loss was thus considered to be due to the removal of parts of silicon/silicon oxides or components of PVDF by the influence of fluorine contained in PVDF ([CH₂CF₂]_n).

Fig. 4 shows the high-resolution transmission electron microscope (HRTEM) micrographs of pure silicon (average particle

size: 1 μm) and the interface between silicon and carbon of the pyrolyzed Si/PVDF composite. From Fig. 4a, one could obviously distinguish the amorphous layer of silicon oxides with a thickness of approximately 2–5 nm on the surface of silicon. This can be explained by considering that pure silicon is easily oxidized under air. The impurities of SiO_x might be involved in the electrochemical reaction due to a strong Si–O bond and consume the intercalated lithium, resulting in an increased irreversible capacity of silicon at the first cycle. The overall picture of the pyrolyzed Si/C composite in Fig. 4b shows that pure silicon was covered by a thick amorphous layer of approximately 20–50 nm, which corresponded to the pyrolyzed PVDF. This micrograph enables us to conclude that the pyrolysis of PVDF could construct a compact interface between carbon and silicon, which is a benefit for providing the electron paths for Si. The strong etching on silicon by fluorine could remove oxygen impurities on the surface of silicon and/or in the disordered carbon. This may accelerate the formation of the inert SiC phases to a certain extent.

Fig. 5 shows the charge and discharge profiles of the pyrolyzed Si/PVDF composite. In the deep Li intercalation below 0.1 V, an extremely flat voltage plateau at the first cycle was obvious owing to an irreversible phase transformation of silicon from crystalline to amorphous. This resulted in an obvious shift in the discharge voltage from the first to the subsequent cycles. A gradual slope observed in the voltage plateau above 0.25 V indicated the disordered carbon. This is in good agreement with the XRD observations. The first efficiency was 77%, which is partially due to the irreversible capacity

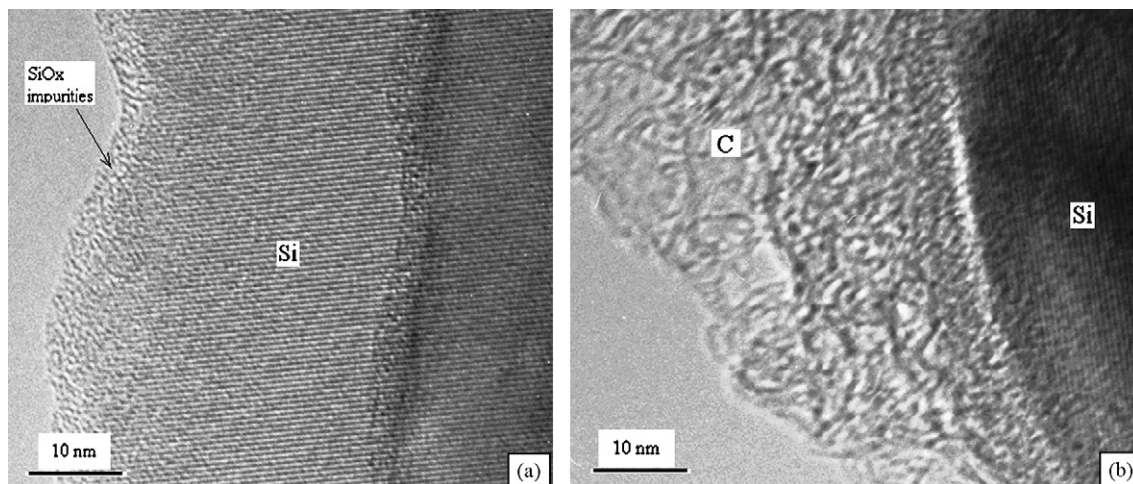


Fig. 4. TEM micrographs of the interface of (a) pure Si (1 μm) and (b) the cross-section of the pyrolyzed Si/PVDF composite at 900 °C.

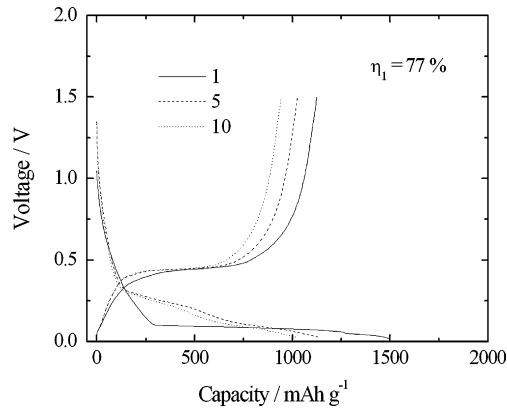


Fig. 5. Charge and discharge profiles of the pyrolyzed Si/PVDF composite at 900 °C at different cycles.

loss of the pyrolyzed PVDF. The pyrolyzed PVDF is a nongraphitizable carbon which shows a reversible capacity of ca. 300 mAh g⁻¹ [18]. After the second cycle, the electrochemical behavior of the composite was dominated by silicon insertion host, suggesting a small quantity of lithium storages in the carbonaceous matrix. The charge and discharge profiles of the pyrolyzed products included in Fig. 1 presented a high comparability due to the contribution of a high capacity of the Li–Si alloying reaction.

Fig. 6 summarizes the cycling performance of the pyrolyzed Si/C composites under potential cutoff at 1.5/0.02 V vs. Li/Li⁺. In order to make a fair comparison, the resulting carbon contents in the pyrolyzed products were almost comparable (ca. 60 wt.%) by selecting a suitable ration of the organic precursors to silicon prior to pyrolysis. The capacity retentions after 16 cycles were 45, 44, 47, 62, 47, 63, 46 and 67% for the pyrolyzed Si–sucrose, Si–resin, Si–PEO, Si–PVC, Si–PE, Si–CPE, Si–pitch and Si–PVDF composites, respectively. Obviously, the morphological stability of the Si/C composite pyrolyzed by PVDF is superior to that by other precursors. Note that the particle size of Si was approximately 1 μm, which was not small sufficient to control the volume changes of Si to a satisfactory degree.

To further improve the morphological stability of Si, ultrafine powders of Si with average size of 60 nm was used for the pyroly-

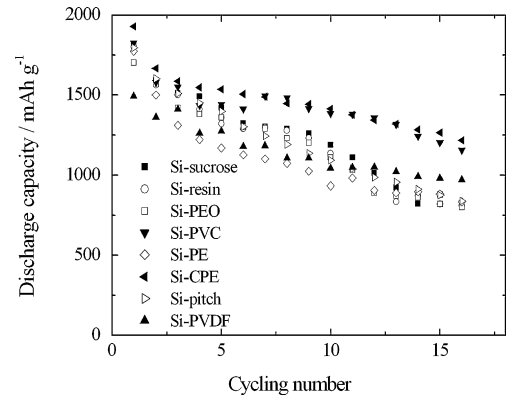


Fig. 6. Cycling performance of the pyrolyzed Si/C composites based on various organic precursors at 900 °C.

sis with PVDF. Fig. 7a shows TEM micrograph of the pyrolyzed Si/PVDF nanocomposite. The pyrolyzed composite presented a highly porous structure which may leave many interspaces to absorb the volume effects of Si during lithium intercalation and extraction. Fig. 7b further shows the high-resolution transmission electron microscope micrograph of the enlarged section of Fig. 7a. Si domains of several nanometers in size were observed and were indicated by the arrowhead. The typical electron-beam diffraction of silicon was showed in inset of Fig. 7b. The original grain size of Si (60 nm) was highly reduced to several nanometers due to the strong etching of fluorine. This helped to maintain the mechanical stability of Si by relieving stresses resulting from Si volume change.

The reversible capacities as a function of cycle number of the pyrolyzed Si/PVDF composite and the nanosized Si were shown in Fig. 8. A rapid drop in capacity occurred within a few cycles for the nanosized pure Si. When the pyrolyzed PVDF was used, a considerable improvement in cycling stability was obtained. 75% capacity retention was observed over 50 cycles with a stable capacity of 660 mAh g⁻¹. Moreover, the coulombic efficiency at the first cycle of 66% for nanosized Si was improved to 75% for the pyrolyzed Si/PVDF composite, suggesting that embedding of nanocluster of Si within the disordered carbon could effectively prevent a direct contact of Si with the electrolyte. The nano-porous structure can successfully

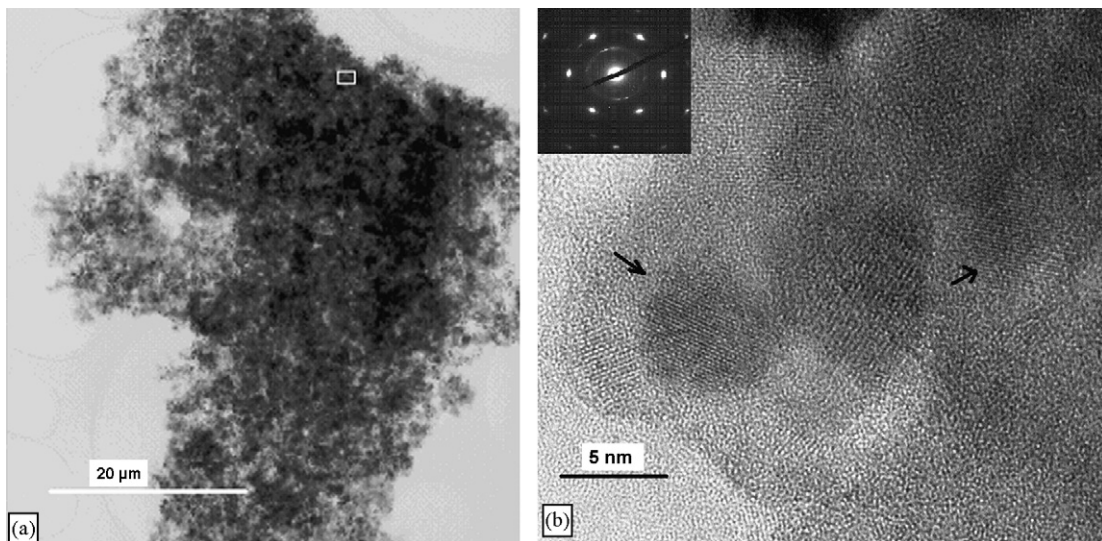


Fig. 7. (a) TEM micrograph of the pyrolyzed Si/PVDF composite and (b) HRTEM micrograph of the enlarged section of (a).

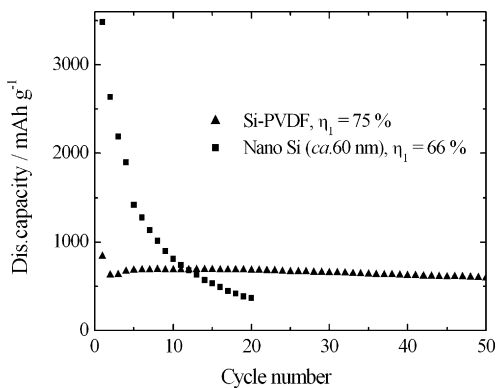


Fig. 8. Cycling performance of the nanosized Si and the pyrolyzed Si/PVDF composite.

suppress the volume change of silicon during the electrochemically alloying process.

4. Conclusion

In this work, we found that pyrolysis of poly(vinylidene fluoride) could provide an appropriate carbon matrix to suppress the pulverizing of Si by the volume changes during lithium intercalation and extraction. This could be attributed to the strong etching of fluorine to silicon during the pyrolysis. This helped constructing of a compact interface between Si and the disordered carbon. Moreover, the Si nanoclusters were uniformly embedded within the pyrolyzed PVDF. This gave an obvious improvement of the cyclability of silicon. The porous nanocomposite exhibited a specific capacity of approximately 660 mAh g^{-1} with a 75% capacity retention after 50 cycles.

Acknowledgements

This work was financially supported by NSFC Project No. 20333040 and 50672114, 863 Project of China No. 2006AA03Z232 and 973 Project of China No. 2007CB209700.

References

- [1] A.M. Wilson, J.N. Reimers, E.W. Fuller, J.R. Dahn, *Solid State Ionics* 74 (1994) 249.
- [2] A.M. Wilson, J.R. Dahn, *J. Electrochem. Soc.* 142 (1995) 326.
- [3] Z.S. Wen, J. Yang, B.F. Wang, K. Wang, Y. Liu, *Electrochem. Commun.* 5 (2003) 165.
- [4] J. Yang, B.F. Wang, K. Wang, Y. Liu, J.Y. Xie, Z.S. Wen, *Electrochem. Solid-State Lett.* 6 (2003) A154.
- [5] I.-S. Kim, P.N. Kumta, *J. Power Sources* 136 (2004) 145.
- [6] G.X. Wang, J.H. Ahn, J. Yao, S. Bewlay, H.K. Liu, *Electrochem. Commun.* 6 (2004) 689.
- [7] X.W. Zhang, P.K. Patil, C. Wang, A.J. Appleby, F.E. Little, D.L. Cocke, *J. Power Sources* 125 (2004) 206.
- [8] Y. Liu, K. Hanai, J. Yang, N. Imanishi, A. Hirano, Y. Takeda, *Solid State Ionics* 168 (2004) 61.
- [9] N. Dimov, K. Fukuda, T. Umeno, S. Kugino, M. Yoshio, *J. Power Sources* 5030 (2002) 1.
- [10] X.Q. Yang, J. McBreen, W.S. Yoon, M. Yoshio, H.Y. Wang, K.J. Fukuda, T. Umeno, *Electrochem. Commun.* 4 (2002) 893.
- [11] N. Dimov, S. Kugino, M. Yoshio, *Electrochim. Acta* 48 (2003) 1579.
- [12] M. Yamada, Y.Y. Xia, A. Ueda, S. Aoyama, *Proceedings of the 44th Battery Symposium in Japan*, P1D12, November 4–6, 2003.
- [13] Y. Liu, K. Hanai, J. Yang, N. Imanishi, A. Hirano, Y. Takeda, *Electrochem. Solid-State Lett.* 7 (2004) A369.
- [14] Y. Liu, K. Hanai, T. Matsumura, N. Imanishi, A. Hirano, Y. Takeda, *Electrochem. Solid-State Lett.* 7 (2004) A492.
- [15] A. Timmons, A.D.W. Todd, S.D. Mead, G.H. Carey, R.J. Sanderson, J.R. Dahn, *J. Electrochem. Soc.* 154 (2007) A865.
- [16] W. Xing, A.M. Wilson, G. Zank, K. Eguchi, J.R. Dahn, *J. Electrochem. Soc.* 144 (1997) 2410.
- [17] C.G. Walle, F.R. McFeely, S.T. Pantelides, *Phys. Rev. Lett.* 61 (1988) 1867.
- [18] T. Zheng, Y.H. Liu, E.W. Fuller, S. Tseng, U.V. Sacken, J.R. Dahn, *J. Electrochem. Soc.* 142 (1995) 2581.